DOI: 10.1002/ejic.201000766

Syntheses, Structures and Properties of a Series of Zn^{II} Complexes Constructed from a Tetrakis(imidazole) Ligand and Various Anions

Hong-Ye Bai,[a] Jian-Fang Ma,*[a] Jin Yang,*[a] Bo Liu,[a] Lai-Ping Zhang,[a] Ji-Cheng Ma,[a] and Ying-Ying Liu[a]

Keywords: Coordination polymers / Zinc / N ligands / Carboxylate ligands / Hydrothermal synthesis

Six new coordination polymers, namely, $[Zn(L)](NO_3)_2{\cdot}3H_2O$ (**1**), $[Zn_2(L)_{0.5}(HPO_3)_2]{\cdot}H_2O$ (**2**), $[Zn_2(L)(L^1)_2]{\cdot}3H_2O$ (**3**), $[Zn_2(L)(L^2)_2]{\cdot}4.75H_2O$ (**4**), $[Zn_2(L)(L^3)_2]{\cdot}3H_2O$ (**5**), and $[Zn_2(L)(L^4)]{\cdot}3H_2O$ (**6**), where L = tetrakis(imidazol-1-ylmethyl)methane, H_2L^1 = oxalic acid, H_2L^2 = 1,3-benzenedicarboxylic acid, H_2L^3 = 5-OH-1,3-benzenedicarboxylic acid, and H_4L^4 = 4,4′-oxydiphthalic acid, were successfully synthesized under hydrothermal conditions. In compound **1**, the L ligands connect the Zn^{II} ions to yield a 3D 4-connected $4{\cdot}6^5$ net with the free NO_3^- filling the channels. In compound **2**, HPO_3^{2-} anions and L ligands link the Zn^{II} centers to generate a pentanodal (3,4)-connected $(4{\cdot}6{\cdot}8)(6^2{\cdot}8)(6^2{\cdot}8^4)(4{\cdot}6{\cdot}8^3{\cdot}10)(8^4{\cdot}10^2)_2$ net. In compound **3**, the $Zn_2L^1{}_2$ units are linked by the L ligands to form a 2D 6^3 network. In compound **4**, the L and L^2 ligands connect the Zn^{II} ions to form a 3D framework with $(4{\cdot}6^2{\cdot}8^3)(6^2{\cdot}7^2{\cdot}8^2)(4{\cdot}6{\cdot}7^3{\cdot}8)$ topology. In compound **5**, L ligands coordinate with the Zn^{II} centers to give a 2D binodal 4-connected layer with the Schläfli symbol of $(5^5{\cdot}8)_2(5^4{\cdot}6^2)$, which are further consolidated by L^3 ligands. In compound **6**, the Zn^{II} centers are connected by the L and L^4 ligands to form a 2D 4-connected $4^3{\cdot}6^3$ network. The structural differences in **1**–**6** suggest the importance of the anions in the construction of the coordination polymers. The compounds underwent thermogravimetric analysis, and the luminescent properties of the compounds were also investigated.

Introduction

Research of the design and synthesis of metal-organic frameworks (MOFs) has attracted much attention from chemists, not only because of the functional properties of these materials, but also because of their fascinating structures and topologies.[1] Up to now, lots of MOFs with interesting structures and topologies have been investigated and reported.[2] However, the controllable synthesis of MOFs is still a great challenge because there are many factors that play important roles in their self-assembly, such as the chemical structures of the ligands, the metal, the anions, reaction temperature and pH value.[3] The selection of the ligand is a vital subject in the construction of MOFs. So far, N-containing rigid polydentate ligands, such as pyrazine, 4,4′-bipyridine, 2,2′-bipyridine, and phenanthroline have been investigated extensively.[4] However, investigations of flexible N-containing polydentate ligands have been lacking.[5] Flexible N-containing polydentate ligands are excellent candidates for the construction of novel intriguing structures and topologies, because they have multiple coordination sites and can adopt versatile conformations.[6]

Recently, we have investigated the coordination chemistry of the flexible tetradentate ligand tetrakis(imidazol-1-ylmethyl)methane (L).[7] The results indicate that ligand L is a good candidate for the construction of coordination polymers with interesting topologies and properties (Scheme 1). As a continuation of the investigation of the tetrakis(imidazole) ligand (L), six Zn^{II} complexes (**1**–**6**) with different structures and topologies were synthesized under hydrothermal conditions. The influence of the counteranions on the coordination ability, flexibility, carboxylate group number, carboxylate group angles, and substitutional groups on the structures is discussed. All the compounds have been characterized by elemental analysis,

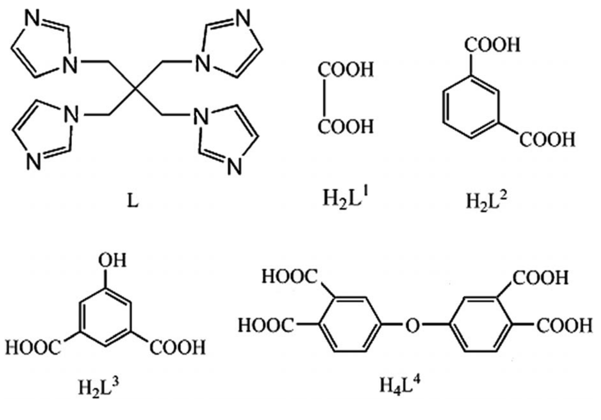

Scheme 1. The L ligand and carboxylate ligands used in this work.

---

[a] Key Lab of Polyoxometalate Science, Department of Chemistry, Northeast Normal University,
Changchun 130024, People's Republic of China
E-mail: jianfangma@yahoo.com.cn
yangjinnenu@yahoo.com.cn

Supporting information for this article is available on the WWW under http://dx.doi.org/10.1002/ejic.201000766.

and X-ray crystallography. The compounds underwent topological analysis and thermogravimetric analyses, and the photoluminescent properties of the materials in the solid state have also been investigated.

Results and Discussion

Structure of [Zn(L)]$(NO_3)_2 \cdot 3H_2O$ (1)

To investigate the effect of inorganic anions on the structures of the coordination polymers, anions NO_3^- and HPO_3^{2-} were applied in syntheses conducted under similar conditions, and compounds **1** and **2** were isolated. The XRD study showed that there is one crystallographically independent Zn^{II} center, one L ligand, two nitrate anions, and three lattice water molecules in the asymmetric unit of **1**. As shown in part a of Figure 1, the Zn^{II} atom is coordinated to four nitrogen atoms from four L ligands and exhibits a tetrahedral ZnN_4 coordination geometry [Zn1–N4$^{\#1}$ 1.974(3), Zn1–N8$^{\#2}$ 1.978(3), Zn1–N1 1.986(3) and Zn1–N6$^{\#3}$ 2.008(3) Å; symmetry codes are given in the legend for Figure 1]. Each L ligand is a tetradentate ligand and connects four Zn^{II} ions through its four imidazole groups to form a 3D framework structure as illustrated in Figure 1 (b). Topologically, the Zn^{II} ions and L ligands can be reduced to 4-connected nodes, so the 3D structure of **1** can be described as a 4-connected net with the Schläfli symbol $4 \cdot 6^5$ (Figure 1, c). The channels are filled with uncoordinated nitrate ions and free water molecules. Two symmetry-related O1W and two symmetry-related O2W water molecules act as both hydrogen bond donors and acceptors to form a cyclic water tetramer (O1W–H1C···O2W and O2W–H2D···O1W$^{\#7}$). Furthermore, each tetramer is linked to four adjacent tetramers by nitrate ions and additional water molecules through O–H···O hydrogen bonds (O1W–H1D···O4, O2W–H2C···O3W$^{\#4}$, O3W–H3C···O3$^{\#8}$, O3W–H3C···O1$^{\#8}$, O3W–H3D···O5) to furnish 2D hydrogen-bonded layers (Figure S1), which stabilize the 3D framework of **1**.

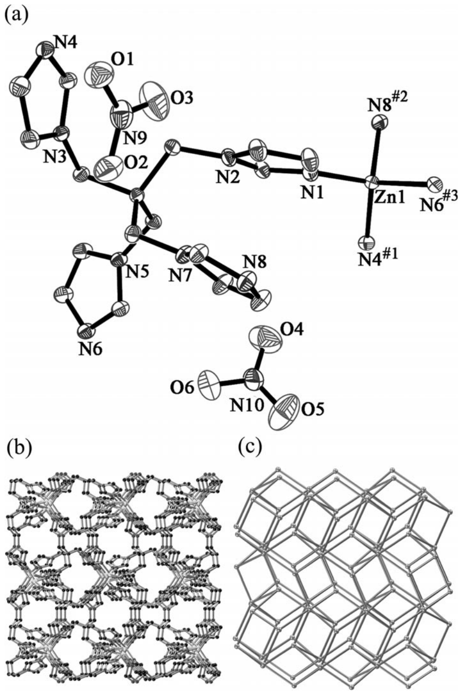

Figure 1. (a) ORTEP view of **1** showing the local coordination environment of the Zn^{II} ions with hydrogen atoms and lattice water molecules omitted for clarity (displacement ellipsoids are drawn at the 30% probability level). Symmetry codes: #1 x, $-y + 1/2$, $z - 1/2$; #2 $-x + 3/2$, $y - 1/2$, z; #3 $x - 1/2$, $-y + 1/2$, $-z + 2$. (b) The 3D structure of **1**. (c) Schemetic representation of the 4-connected net of **1** with the Schläfli symbol $(4 \cdot 6^5)$.

Structure of $[Zn_2(L)_{0.5}(HPO_3)_2] \cdot H_2O$ (2)

In order to investigate the effect of the inorganic anion on the complex structure, the reaction of L, H_3PO_3, and $ZnCO_3$ under similar condition as used to prepare compound **1** was carried out, and a new complex **2** with a 3D structure was successfully isolated. As shown in part a of Figure 2, the asymmetric unit of **2** contains two crystallographically independent Zn^{II} ions (Zn1 and Zn2), half a L ligand, two kinds of phosphite anions, and one lattice water

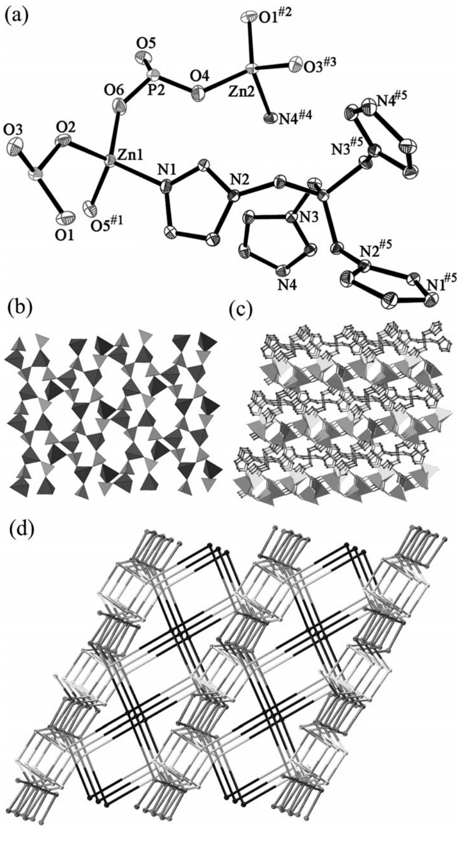

Figure 2. (a) ORTEP view of **2** showing the local coordination environment of the Zn^{II} ions with hydrogen atoms and lattice water molecules omitted for clarity (displacement ellipsoids are drawn at the 30% probability level). Symmetry codes: #1 $-x + 1/2$, $y - 1/2$, $-z + 3/2$; #2 x, $y + 1$, z; #3 $-x + 1/2$, $-y + 1/2$, $-z + 1$; #4 $-x$, $-y + 1$, $-z + 1$. (b) The 2D inorganic layer constructed from HPO_3^{2-} and Zn^{II} ions. (c) The 3D framework of compound **2**. (d) Schemetic representation of the (3,4)-connected net of **2** with Schläfli symbol $(4 \cdot 6 \cdot 8)(6^2 \cdot 8)(6^2 \cdot 8^4)(4 \cdot 6 \cdot 8^3 \cdot 10)(8^4 \cdot 10^2)_2$.

molecule. Each Zn^{II} center is four-coordinate, and is connected to one nitrogen atom from one L ligand and three oxygen atoms from three HPO_3^{2-} anions, and have tetrahedral ZnO_3N coordination spheres [Zn1–N1 2.004(3), Zn1–O2 1.952(3), Zn1–O6 1.925(3), Zn1–$O5^{\#1}$ 1.940(3), Zn2–$N4^{\#4}$ 2.019(4), Zn2–$O1^{\#2}$ 1.915(3), Zn2–$O3^{\#3}$ 1.958(3) and Zn2–O4 1.946(3) Å; symmetry codes are given in the legend for Figure 2]. Zinc tetrahedra (ZnO_3N) and phosphorus-tetrahedra (HPO_3^-) are connected to each other, forming a 2D inorganic layer with 4-, 6- and 8-membered rings (Figure 2, b). Topologically, the layer can be simplified to a 3-connected 2D net with $(4\cdot6\cdot8)(6^2\cdot8)$ topology. The 2D inorganic layer is quite different from the previously reported zinc phosphate frameworks that form in the presence of neutral N-containing ligands.[8] Furthermore, each L ligand coordinates to two Zn1 and two Zn2 ions in a tetradentate coordination mode, connecting the 2D layers to form a 3D structure (Figure 2, c).

From a topological point of view, if the Zn1 and Zn2 ions and the L ligands are viewed as three kinds of 4-connected nodes, and the two types of HPO_3^- anions are considered as two kinds of 3-connected nodes, the 3D framework of **2** becomes a pentanodal (3,4)-connected net with Schläfli symbol $(4\cdot6\cdot8)(6^2\cdot8)(6^2\cdot8^4)(4\cdot6\cdot8^3\cdot10)(8^4\cdot10^2)_2$ (Figure 2, d).

Structure of $[Zn_2(L)(L^1)_2]\cdot3H_2O$ (3)

Multicarboxylate ligands are powerful ligands for the construction of coordination polymers with diverse structures owing to their various coordination modes. To explore the effect of multicarboxylate ligands on the formation of these complexes, four kinds of multicarboxylate ligands H_2L^1, H_2L^2, H_2L^3, and H_4L^4 were used. When the organic ligand oxalic acid (H_2L^1) was used instead of H_3PO_3 under the same condition used to prepare compound **2**, a structurally different compound, **3**, was obtained. As shown in Figure 3 (a), the asymmetric unit of compound **3** consists of two kinds of Zn^{II} centers (Zn1 and Zn2), one L ligand, and two kinds of L^1 ligands. The Zn1 ion is five-coordinate and is bound to one nitrogen atom from one L ligand and four oxygen atoms from two L^1 ligands [Zn1–N1 2.032(4), Zn1–O7 1.994(3), Zn1–O5 2.005(3), Zn1–O4 2.071(3), and Zn1–O2 2.136(3) Å] in a distorted tetragonal pyramid arrangement. The Zn2 ion is five-coordinate, and is connected to three nitrogen atoms from three L ligands and two oxygen atoms from one L^1 anion [Zn2–$N8^{\#1}$ 2.046(3), Zn2–N4 2.049(4), Zn2–$N6^{\#2}$ 2.074(3), Zn2–O1 2.105(3), and Zn2–O3 2.135(3) Å; symmetry codes are given in the legend for Figure 3]. The L^1 ligands show different coordination modes in this complex. One L^1 ligand coordinates to one Zn1 ion in a chelating coordination mode (L^1A), while another L^1 ligand coordinates to both Zn1 and Zn2 in a bis-chelating coordination mode (L^1B). The L^1A and L^1B ligands connect the Zn1 and Zn2 ions into a $Zn_2L^1_2$ unit. Further, the L ligands link the $Zn_2L^1_2$ units to form a 2D layer (Figure 3, b). From a topological view point, the L lsidered as a three-connected node, and the 2D structure of compound **3** is simplified to a 3-connected 6^3 network (Figure 3, c).

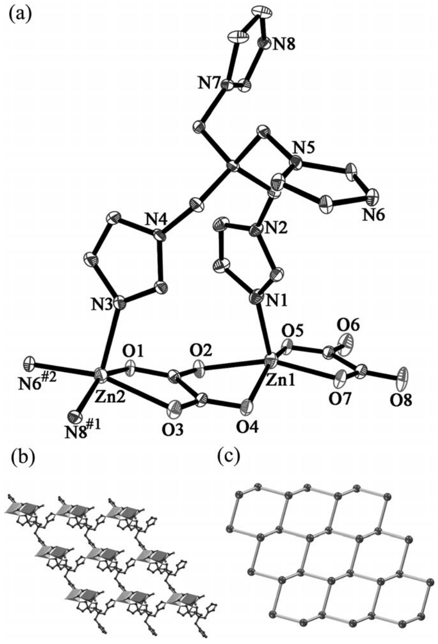

Figure 3. (a) ORTEP view of **3** showing the local coordination environment of the Zn^{II} ions with hydrogen atoms and lattice water molecules omitted for clarity (displacement ellipsoids are drawn at the 30% probability level). Symmetry codes: #1 $x + 1, y - 1, z$; #2 $x, y - 1, z$; #3 $x, y + 1, z$. (b) The 2D framework of compound **3**. (c) Schemetic representation of the 6^3 net of compound **3**.

Structure of $[Zn_2(L)(L^2)_2]\cdot4.75H_2O$ (4)

To evaluate the effect of the dicarboxylate ligand spacer on the framework formation of the polymer complex, the H_2L^2 ligand with a phenyl spacer group was reacted, instead of H_2L^1, with $ZnCO_3$ and L, using a preparation procedure similar to that used to prepare **3**. The XRD study showed that there are two crystallographically independent Zn^{II} centers, two kinds of crystallographically independent ligands, and one kind of L ligand in the asymmetric unit of **4**. As shown in Figure 4 (a), both Zn1 and Zn2 ions are four-coordinate, and are bound to two nitrogen atoms [Zn1–N1 2.007(5), Zn1–$N8^{\#1}$ 2.011(5), Zn2–$N5^{\#2}$ 2.005(5) and Zn2–$N3^{\#3}$ 2.009(5) Å; symmetry codes are given in the legend for Figure 4] from two L ligands and two carboxylate oxygen atoms from two different L^2 ligands [Zn1–O2 1.982(3), Zn1–O6 1.987(4), Zn2–O3 1.966(4) and Zn2–$O7^{\#4}$ 2.042(3) Å; symmetry codes are given in the legend for Figure 4] in a tetrahedral coordination environments. The L^2 ligands link the Zn^{II} ions (Zn1 and Zn2) to form a 1D chain with two different Zn···Zn distances [9.918(2) and 9.987(2) Å] (Figure 4, b). Each L ligand coordinates to two symmetry related Zn1 and two symmetry related Zn2 ions to generate a 2D layer (Figure 4, c), which is further linked by the L^2 ligands to construct a 3D framework (Figure 4, d). Better insight into such an intricate framework can be accessed by reducing the multidimensional structures to simple node-and-connecting nets. The Zn1, Zn2 and the L ligand can be viewed as three kinds of 4-connected nodes, meanwhile the L^2 ligand can be viewed as a linker, so the 3D framework of **4** can be simplified to a trinodal 4-connected net with the Schläfli symbol $(4{\cdot}6^2{\cdot}8^3)(6^2{\cdot}7^2{\cdot}8^2)(4{\cdot}6{\cdot}7^3{\cdot}8)$ (Figure 4, e). Moreover, O–H···O hydrogen bonds exist among the lattice water molecules and the carboxylate oxygen atoms (O1W–H1C···O5, O1W–H1D···O4, O2W–H2D···O2, O2W–H2C···O4W, O3W–H3C···O1W, O3W–H3D···O6W, O4W–H4C···O7W, and O5W–H5C···O8W), which contribute to the stability of the 3D structure.

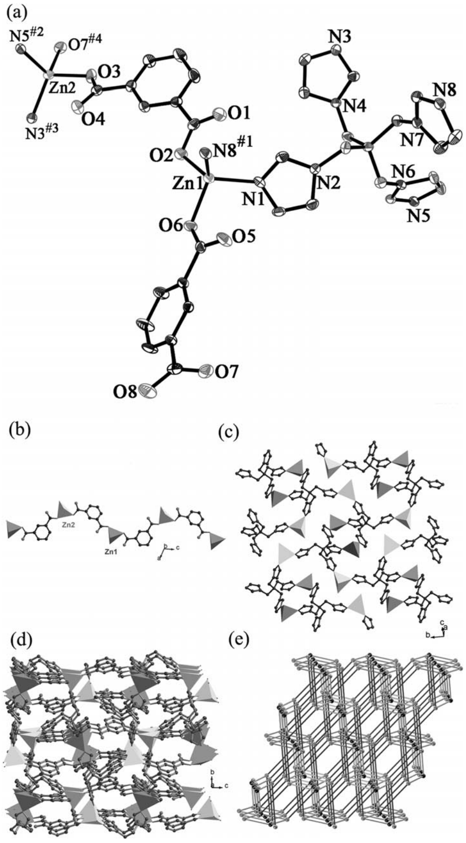

Figure 4. (a) ORTEP view of **4** showing the local coordination environment of the Zn^{II} ions with hydrogen atoms and lattice water molecules omitted for clarity (displacement ellipsoids are drawn at the 30% probability level). Symmetry codes: #1 $-x + 1, -y, -z + 1$; #2 $-x + 3/2, y - 1/2, -z + 1/2$; #3 $x + 1, y, z$; #4 $x, y, z - 1$. (b) The 1D zigzag chain constructed from L^2 ligands and Zn^{II} ions. (c) The 2D wave-like layer constructed from L ligands and Zn^{II} ions. (d) The 3D framework of compound **4**. (e) Schemetic representation of the trinodal 4-connected net of **4** with the Schläfli symbol $(4{\cdot}6^2{\cdot}8^3)(6^2{\cdot}7^2{\cdot}8^2)(4{\cdot}6{\cdot}7^3{\cdot}8)$.

Structure of $[Zn_2(L)(L^3)_2]{\cdot}3H_2O$ (5)

To examine the influence of substituted groups on the complex structure, H_2L^3 with an additional –OH at the 5-position of the benzene ring was used instead of H_2L^2, and a structurally different complex, **5**, was obtained. The asymmetric unit of **5** contains two crystallographically independent Zn^{II} ions (Zn1 and Zn2), one L ligand, two kinds of L^3 (L^3A and L^3B) anions and three lattice water molecules. As shown in Figure 5 (a), each Zn^{II} ion is coordinated to two nitrogen atoms from two L ligands [Zn1–N1$^{\#1}$ 2.005(4), Zn1–N3 2.037(4), Zn2–N6$^{\#3}$ 2.002(4) and Zn2–N7 2.017(4) Å; symmetry codes are given in the legend for Figure 5] and two oxygen atoms from two L^2 ligands [Zn1–O1 1.980(3), Zn1–O4$^{\#2}$ 2.015(4), Zn2–O6$^{\#4}$ 2.017(3) and Zn2–O9 2.022(3) Å; symmetry codes are given in the legend for Figure 5], and exhibit distorted ZnN_2O_2 tetrahedral coordination geometries. The L^3A ligands link to the Zn1 ions in a bidentate mode to form a 1D chain along the *b*-axis with a Zn···Zn distance of 10.291 Å, while the L^3B ligands bridge the Zn2 ions to form a similar chain along the *a*-axis with a Zn···Zn distance of 10.249 Å (Figure 5, b). The two kinds of chain span two different directions showing a grid-like packing mode. Each L ligand coordinates to two symmetry related Zn1 and two symmetry related Zn2 ions to form a 2D layer (Figure 5, c), which are further linked by L^3 ligands via Zn–O bonds (Figure 5, d). From a topological view point, if the L ligands and the Zn^{II} centers are

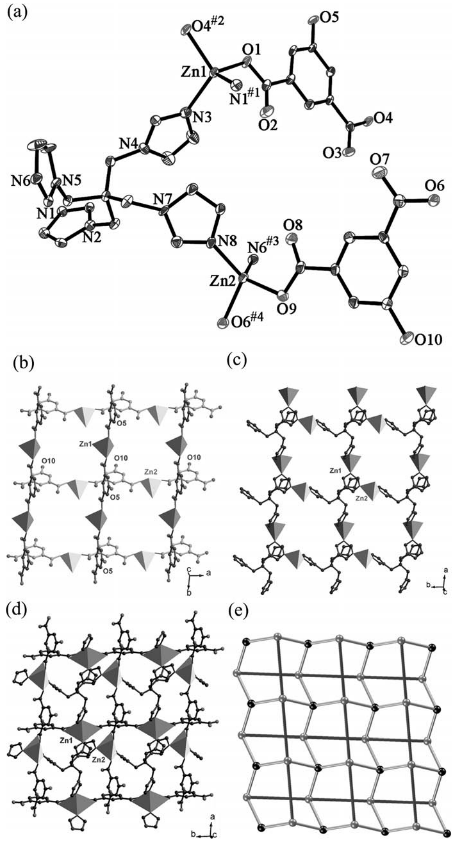

Figure 5. (a) ORTEP view of **5** showing the local coordination environment of the Zn^{II} ions with hydrogen atoms and lattice water molecules omitted for clarity (displacement ellipsoids are drawn at the 30% probability level). Symmetry codes: #1 $x + 1, y, z$; #2 $x, y + 1, z$; #3 $x, y - 1, z$; #4 $x - 1, y, z$. (b) The 1D chain constructed from L^3 ligands and Zn^{II} ions. (c) The 2D layer constructed from L ligands and Zn^{II} ions. (d) The 2D layer of compound **5**. (e) Schemetic representation of the binodal 4-connected net of **5** with the Schläfli symbol $(5^5{\cdot}8)_2(5^4{\cdot}6^2)$.

considered as four-connected nodes, and the L^3 ligands are viewed as linkers, the 2D structure of **5** becomes a binodal 4-connected net with the Schläfli symbol $(5^5{\cdot}8)_2(5^4{\cdot}6^2)$ (Figure 5, e). Furthermore, O–H···O hydrogen bonding interactions exist (O5–H5···O2W, O10–H10···O5, O1W–H1C···O2, and O2W–H2C···O7) that link the 2D layers to form a 3D supramolecular network (Figure S2).

Structure of $[Zn_2(L)(L^4)]{\cdot}3H_2O$ (6)

Different from the rigid dicarboxylates H_2L^1–H_2L^3, the flexible tetracarboxylate ligand H_4L^4 was reacted with $ZnCO_3$ and L under similar reaction condition as used to prepare **3**–**5**, and a new 2D complex **6** was obtained. The asymmetric unit of **6** consists of two crystallographically independent Zn^{II} ions (Zn1 and Zn2), one L ligand, one kind of L^4 ligand, and three lattice water molecules. As shown in Figure 6 (a), both Zn1 and Zn2 ions show distorted tetrahedral coordination environments. Zn1 is four-coordinate, and is connected to three nitrogen atoms from three L ligands, and one oxygen atom from one L^4 ligand [Zn1–O2 1.930(4), Zn1–N6 1.987(4), Zn1–$N1^{\#1}$ 1.990(4) and Zn1–$N8^{\#2}$ 2.008(5) Å; symmetry codes are given in the legend for Figure 6]. Zn2 is four-coordinate, and is bound to one nitrogen atom from one L ligand, and three oxygen atoms from three L^4 anions [Zn2–$O10^{\#3}$ 1.926(4), Zn2–$O7^{\#4}$ 1.965(4), Zn2–O4 1.966(4), and Zn2–$N4^{\#5}$ 2.008(4) Å; symmetry codes are given in the legend for Figure 6]. Each L^4 ligand, in a tetradentate coordination mode, links one Zn1 center and three symmetry related Zn2 centers to furnish a 1D chain along the *a*-axis (Figure 6, b). Each L ligand connects three symmetry related Zn1 centers and one Zn2 center to form a 1D chain along the *a*-axis (Figure 6, c). The two kinds of chains are further connected by shared Zn^{II} centers to generate a 2D layer parallel to the *ac*-plane (Figure 6, d). Topologically, if the L ligands, L^4 ligands and Zn^{II} cations are considered to be 4-connected nodes, the 2D layer of compound **6** can be viewed as a 4-connected net with the Schläfli symbol $(4^3{\cdot}6^3)$ (Figure 6, e). Some hydrogen bonds may exist in compounds **6** based on the O–O distance between the lattice water molecules and the carboxylate oxygen atoms, but no suitable hydrogen atoms were located in the difference Fourier maps for the lattice water molecules.

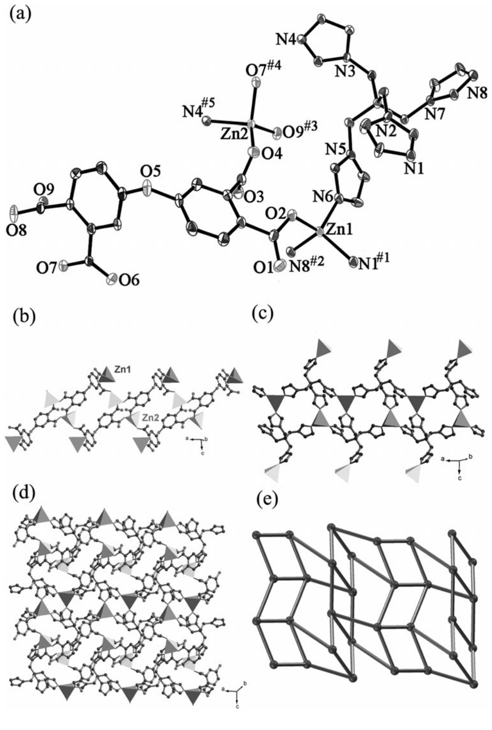

Figure 6. (a) ORTEP view of **6** showing the local coordination environment of the Zn^{II} ions with hydrogen atoms and lattice water molecules omitted for clarity (displacement ellipsoids are drawn at the 30% probability level). Symmetry codes: #1 $-x + 2$, $-y + 1$, $-z + 1$; #2 $x - 1$, y, z; #3 $-x + 1$, $-y + 1$, $-z$; #4 $x + 1$, y, z; #5 $-x + 2$, $-y + 1$, $-z$. (b) The 1D chain constructed from L^4 ligands and Zn^{II} ions. (c) The 1D chain constructed from L ligands and Zn^{II} ions. (d) The 2D layer of compound **6**. (e) Schemetic representation of the 4-connected net of **6** with the Schläfli symbol $(4^3{\cdot}6^3)$.

The Effect of the Counteranions on the Structure of the Complexes

Although the Zn^{II} containing compounds **1**–**6** are all based on tetrakis(imidazole) ligands and were synthesized under similar reaction conditions, they show quite distinct structures and topologies (Scheme 2). This clearly demonstrates that the anions play a crucial role in the formation of these MOFs.

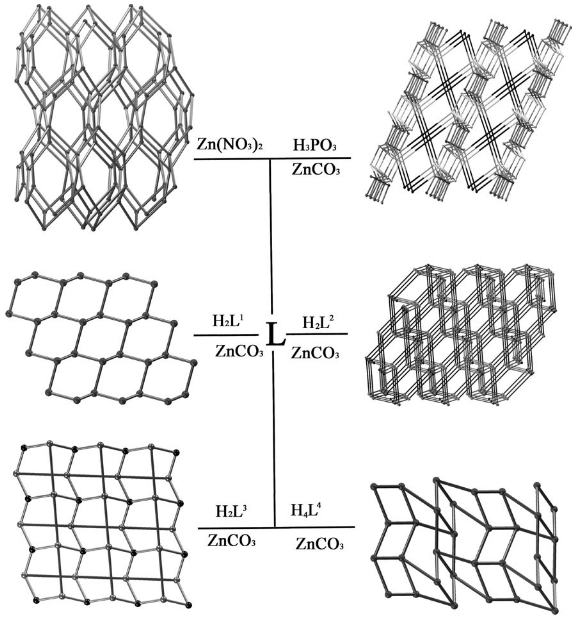

Scheme 2. The structurally different Zn^{II} compounds constructed from tetrakis(imidazole) ligands and various anions.

Compounds **1** and **2**, and our previously reported compound $[Zn_2(L)(SO_4)_2]_3{\cdot}2H_2O$ (**7**)[7b] show the influence of inorganic anions on the formation of the coordination polymers. Compared with the HPO_3^{2-} and SO_4^{2-} anions, the NO_3^- anion has relatively weak coordination ability. As a result, in compound **1**, NO_3^- anions just act as uncoordinated free anions, but in compounds **2** and **7**, the HPO_3^{2-} and SO_4^{2-} anions coordinate to the Zn^{II} centers. In addition, although both HPO_3^{2-} and SO_4^{2-} anions coordinate to the metal centers in compounds **2** and **7**, they show different coordination modes. The HPO_3^{2-} ion coordinates to three Zn^{II} centers in a μ_3-bridging coordination mode to generate a 2D layer in compound **2**, whereas the SO_4^{2-} ion coordinates to two Zn^{II} centers in a μ_2-bridging coordination mode to form a $Zn_2(SO_4)_2$ unit in compound **7**. As mentioned above, the structural discrepancies between **1**, **2** and **7** highlight the effect of the coordination ability of the anion on the framework formation of the complexes. The structural differences between compounds **2** and **7** highlight the effect of the coordination mode of the anions on the coordination polymer structure.

In compounds **3**–**6** four kinds of multicarboxylate ligands (H_2L^1, H_2L^2, H_2L^3 and H_4L^4) were utilized to investigate the effect of the organic ligands on the complex structures. The structural differences between compounds **3** and **4** show the influence of the carboxylate ligand spacer on the framework structures. The two carboxylate groups of L^1 are connected by a C–C bond, whereas those of L^2 are bridged by a phenyl group. The L^1 and L ligands bridge the Zn^{II} centers to furnish the 2D 6^3 network of compound **3**, while L^2 and L ligands link the Zn^{II} centers to form a intricate 3D framework in **4**. The structural differences caused by the carboxylate ligand spacer can also be seen in the different structures of compounds **6** and $[Zn_2(L)(L^7)]_3\cdot 4H_2O$ (**8**)[7b] (H_4L^7 = 1,2,4,5-benzenetetracarboxylic acid). Although both L^4 and L^7 are tetracarboxylate ligands, the spacer of L^4 is longer and more flexible than the phenyl spacer group of L^7. The different spacers for these two tetracarboxylate ligands may be the main reason why there are dimensional differences between compounds **6** and **8**. Substituted groups also plays an important role in the formation of coordination polymer structures. Compared with ligand L^2, ligand L^3 has an additional –OH group at the 5-position of the benzene ring. Possibly, the strong steric hindrance caused by this –OH group hinders the formation of stuctures with high dimensionality. Consequently, in compound **5**, the L^3 and L ligands link the Zn^{II} ions to generate a 2D binodal 4-connected $(5^5\cdot 8)_2(5^4\cdot 6^2)$ net. In addition, the carboxylate group number has a crucial effect on the construction of the complex framework. Compared with the rigid carboxylate ligands L^1, L^2 and L^3, ligand L^4 is a flexible tetracarboxylate ligand. In compound **6**, the tetradentate L^4 and L ligands link the Zn^{II} centers to form a 2D $4^3\cdot 6^3$ network. Notably, although both **3** and **5** have 2D structures, the topology of **6** is entirely different from them. Moreover, the structures of **4** and our previously reported complex $[Zn_2(L)(L^8)_2]\cdot 3.5H_2O$ (**9**)[7b] (H_2L^8 = 1,2-benzenedicarboxylic acid) demonstrate that the angles of the two carboxylate groups also have a significant influence on the final structures. For the rigid dicarboxylate ligands L^2 and L^8, the angles of the two carboxylate groups are 60° and 120°, respectively. Relative to L^2, the smaller angle of L^8 leads to the formation of $Zn_2(L^8)_2$ units, which then results in the structural differences observed between compounds **4** and **9**.

Thermal Analysis

To estimate the stability of compounds **1**–**6** TGA were carried out in a flowing N_2 atmosphere with a heating rate of 10 °C/min^{-1} over the temperature range 50-800 °C (Figure S3 in the SI). For compound **1**, the weight loss before 226 °C is attributable to the loss of water (obsd 7.8 %, calcd. 9.31 %), and the organic ligands began to decompose at 342 °C, leading to the formation of ZnO (obsd. 16.2 %, calcd. 14.03 %). Compound **2** lost water from 50 to 117 °C (obsd. 2.6 %, calcd. 3.77 %), and the anhydrous compound collapsed at 338 °C. For compound **3**, the release of water happened before 204 °C (obsd. 9.1 %, calcd. 7.76 %), and the organic component decomposed at 334 °C. For compound **4**, the first weight loss corresponding to the release of water is observed before 267 °C (obsd 8.8 %, calcd. 6.14 %), and the weight loss from 339 to 673 °C is assigned to the decomposition of the organic ligands. The TGA curve of compound **5** suggests that the first weight loss before 126 °C is attributable to the expulsion of the free water (obsd. 5.7 %, calcd. 6.13 %). The anhydrous framework was stable up to 282 °C, and the remaining weight loss may correspond to the formation of ZnO (obsd 19.4 %, calcd. 18.47 %). For compound **6**, water was lost between 50–153 °C (obsd. 7.3 %, calcd. 8.29 %), and the organic ligands began to decompose at 277 °C.

Photoluminescence of Complexes 1–6

The photoluminescence of d^{10} metal complexes has attracted intensive research interest, owing to their potential application in chemical sensors and photochemistry.[9] To examine the photoluminescent properties of complexes **1**–**6**, their solid state luminescence spectra were collected at room temperature under the same experimental conditions (Figure 7). Ligand L shows emission at about 435 nm with the excitation peak at 365 nm, which may be attributed to $\pi^* \rightarrow \pi$ transitions.[10] The carboxylate ligands H_2L^2 (λ_{ex} = 355 nm, λ_{em} = 403 nm), H_2L^3 (λ_{ex} = 346 nm, λ_{em} = 390 nm) and H_4L^4 (λ_{ex} = 300 nm, λ_{em} = 415 nm) also exhibit fluorescence, which can be assigned to the $\pi^* \rightarrow n$ transition as previously reported.[11] Compounds **1**–**6** exhibit emissions at about 435 nm for **1** (λ_{ex} = 365 nm), at 393 nm (λ_{ex} = 294 nm) for **2**, at 367 nm (λ_{ex} = 291 nm) for **3**, at 404 nm (λ_{ex} = 308 nm) for **4**, at 401 nm (λ_{ex} = 341 nm) for **5**, and at 425 nm (λ_{ex} = 350 nm) for **6**. The solid state luminescence of the Zn^{II} compounds **1**–**6** may be attributed to intraligand charge transfer involving the coordinated L ligand, which is similar to that of the free tetrakis(imidazole) ligand. The carboxylate ligands contribute very little to the fluorescent emission since the fluorescent emission from the $\pi^* \rightarrow n$

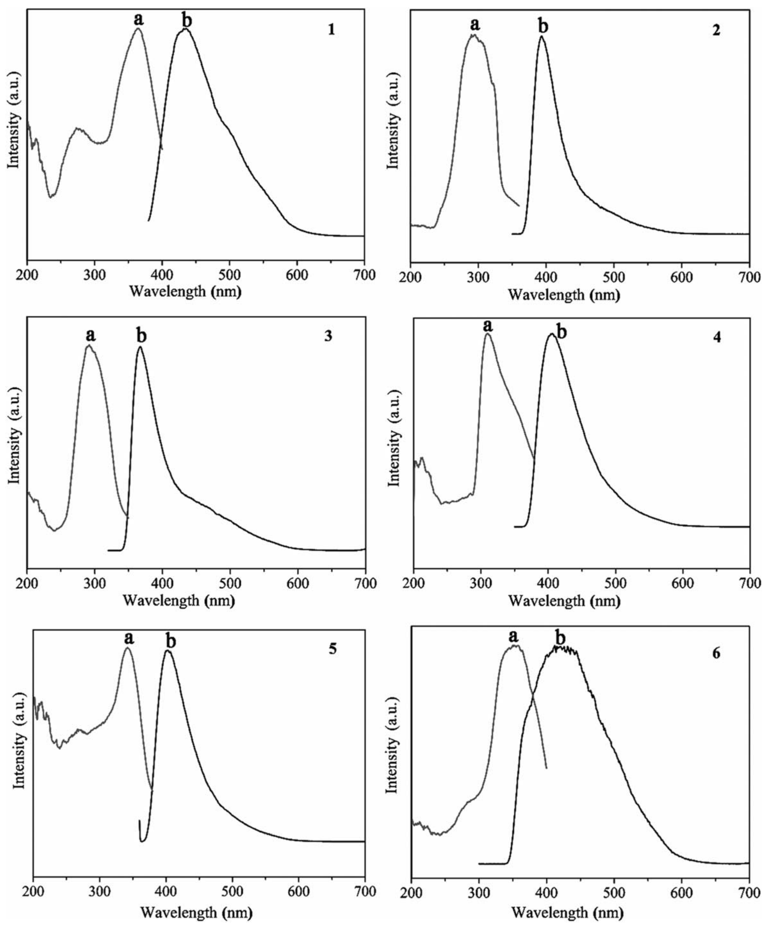

Figure 7. Photoluminescence excitation (a) and emission spectra (b) for compounds **1**–**6** recorded at room temperature.

transition is very weak compared to the π*→π transition for L.[12]

Conclusions

Six new Zn^{II} complexes based on tetrakis(imidazole) ligands and different anions (NO_3^-, HPO_3^{2-}, H_2L^1, H_2L^2, H_2L^3, and H_2L^4) have been synthesized and characterized. The influence of the anions on the structures of the complexes has been investigated. The structural differences imply that different anions can be utilized to adjust the structure of the frameworks and the topologies of the coordination polymers. The luminescent properties of the compounds indicate that they may be good candidates for luminescent materials.

Experimental Section

Materials and Physical Measurements: The ligand tetrakis(imidazol-1-ylmethyl)methane (L) was prepared according to a literature procedure.[7a] All other reagents and solvents were purchased from commercial sources and used without further purification. The C,H,N elemental analyses were conducted on a Perkin–Elmer 240C elemental analyzer. The FT-IR spectra were recorded from KBr pellets in the range 4000–400 cm^{-1} on a Mattson Alpha-Centauri spectrometer. The photoluminescent properties of the ligands and compounds were measured on a Perkin–Elmer FLS-920 spectrometer. TGA were performed on a Perkin–Elmer TG-7 analyzer heated from 50 to 800 °C under nitrogen. Powder XRD patterns of the samples were collected on a Rigaku Dmax 2000 X-ray diffractometer with graphite-monochromatized Cu-K_α radiation (λ = 0.154 nm) in the 2θ range of 5 to 50°. The experimental powder XRD patterns are in good agreement with the corresponding simulated ones (Figure S4 in the Supporting Information) except for the relative intensity variation due to the preferred orientation of the crystals. Therefore, the phase purity of the as-synthesized products has been confirmed.

Synthesis of $[Zn(L)](NO_3)_2\cdot 3H_2O$ (1): A mixture of L (16.8 mg, 0.05 mmol), $Zn(NO_3)_2\cdot 6H_2O$ (29.75 mg, 0.10 mmol), and water (10 mL) was placed in a Teflon® reactor (15 mL) and heated at 150 °C for 3 d. After the mixture had been cooled to room temperature at a rate of 10 °C h^{-1}, colorless crystals of **1** were obtained with a yield of 47% (based on L). $C_{17}H_{26}N_{10}O_9Zn$ (M_r = 579.85): calcd. C 35.21, H 4.52, N 24.16; found C 35.47, H 4.36, N 24.31. IR: $\tilde{\nu}$ = 3439 (m), 3123 (m), 3054 (w), 2939 (w), 1636 (w), 1531 (m), 1460 (w), 1353 (s), 1246 (m), 11099 (s), 1026 (w), 954 (m), 847 (w), 829 (w), 756 (m), 655 (s), 627 (m), 555 (w), 508 (w) cm^{-1}.

Synthesis of $[Zn_2(L)_{0.5}(HPO_3)_2]\cdot H_2O$ (2): A mixture of $ZnCO_3$ (12.5 mg, 0.10 mmol), H_3PO_3 (82.0 mg, 0.10 mmol), L (16.8 mg, 0.05 mmol), and water (10 mL) was placed in a Teflon® reactor (15 mL) and heated at 150 °C for 3 d. After the mixture had been cooled to room temperature at a rate of 10 °C h^{-1}, colorless crystals of **2** were obtained (64% yield based on $ZnCO_3$). $C_{8.50}H_{14}N_4O_7P_2Zn_2$ (M_r = 476.92): calcd. C 21.40, H 2.96, N 11.75; found C 21.28, H 3.07, N 11.86. IR: ṽ = 3536 (w), 3443 (m), 3154 (w), 3120 (s), 3023 (w), 2965 (w), 2921 (w), 2425 (s), 2400 (s), 1656 (s), 1536 (s), 1453 (m), 1440 (w), 1300 (w), 1251 (m), 1148 (w), 1112 (m), 1074 (m), 1012 (m), 951 (s), 924 (w), 855 (m), 773 (s), 658 (s), 629 (m), 588 (w), 470 (w) cm^{-1}.

Synthesis of $[Zn_2(L)(L^1)_2]\cdot 3H_2O$ (3): The preparation method for **3** was similar to that of **2** except that H_2L^1 (0.10 mmol) was used instead of H_3PO_3. Colorless crystals of **3** were collected in a 73% yield (based on $ZnCO_3$). $C_{21}H_{25}N_8O_{11}Zn_2$ (M_r = 696.23): calcd. C 36.22, H 3.62, N 16.09; found C 36.18, H 3.74, N 16.16. IR: ṽ = 3404 (s), 3132 (m), 3105 (s), 2986 (w), 1646 (s), 1606 (s), 1516 (m), 1402 (w), 1365 (w), 1312 (m), 1238 (m), 1112 (m), 1089 (s), 1026 (w), 941 (m), 864 (w), 797 (s), 736 (w), 663 (s), 624 (m), 495 (m) cm^{-1}.

Synthesis of $[Zn_2(L)(L^2)_2]\cdot 4.75H_2O$ (4): The preparation method for **4** was similar to that of **2** except that H_2L^2 (0.10 mmol) was used instead of H_3PO_3. Colorless crystals of **4** were collected in a 65% yield (based on $ZnCO_3$). $C_{33}H_{37.50}N8O_{12.75}Zn_2$ (M_r = 880.95): calcd. C 44.99, H 4.29, N 12.72; found C 45.06, H 4.17, N 12.84. IR: ṽ = 3668 (m), 3435 (w), 3144 (m), 3116 (m), 1609 (s), 1570 (m), 1525 (m), 1456 (w), 1387 (m), 1347 (s), 1297 (w), 1251 (m), 1159 (w), 1105 (s), 1048 (s), 1048 (w), 1028 (m), 951 (s), 906 (m), 836 (m), 743 (s), 722 (m), 658 (s), 629 (w), 534 (w), 471 (w) cm^{-1}.

Synthesis of $[Zn_2(L)(L^3)_2]\cdot 3H_2O$ (5): The preparation method for **5** was similar to that of **2** except that H_2L^3 (0.10 mmol) was used instead of H_3PO_3. Colorless crystals of **5** were collected in a 79% yield (based on $ZnCO_3$). $C_{33}H_{34}N_8O_{13}Zn_2$ (M_r = 881.42): calcd. C 44.96, H 3.89, N 12.71; found C 45.14, H 4.06, N 12.93. IR: ṽ = 3381 (w), 3136 (w), 1623 (w), 1522 (m), 1379 (s), 1298 (w), 1250 (w), 1114 (w), 1099 (w), 1026 (w), 971 (m), 892 (w), 836 (m), 801 (m), 779 (m), 656 (m), 624 (w) cm^{-1}.

Synthesis of $[Zn_2(L)(L^4)]\cdot 3H_2O$ (6): The preparation method for **6** was similar to that of **2** except that H_4L^4 (0.05 mmol) was used instead of H_3PO_3. Colorless crystals of **6** were collected in a 63% yield (based on $ZnCO_3$). $C_{33}H_{37}N_8O_{12}Zn_2$ (M_r = 868.45): calcd. C 45.64, H 4.29, N 12.90; found C 45.46, H 4.13, N 12.77. IR: ṽ = 3422 (w), 3126 (w), 1564 (w), 1522 (w), 1380 (s), 1295 (w), 1260 (w), 1227 (m), 1147 (w), 1110 (s), 1026 (w), 951 (s), 837 (s), 769 (w), 655 (s), 626 (w), 514 (w) cm^{-1}.

Table 1. Crystal data and structure refinement details for compounds **1**–**6**.

	1	**2**	**3**
Empirical formula	$C_{17}H_{26}N_{10}O_9Zn$	$C_{8.50}H_{14}N_4O_7P_2Zn_2$	$C_{21}H_{25}N_8O_{11}Zn_2$
Formula weight	579.85	476.92	696.23
Crystal system	orthorhombic	monoclinic	triclinic
Space group	*Pbca*	*C*2/*c*	$P\bar{1}$
a [Å]	18.295(5)	22.339(5)	10.661(5)
b [Å]	14.541(5)	9.697(5)	10.935(5)
c [Å]	18.655(5)	15.663(5)	12.624(5)
α [°]	90	90	84.683(5)
β [°]	90	116.931(5)	87.190(5)
γ [°]	90	90	63.678(5)
V [Å^3]	4963(3)	3025(2)	1313.4(10)
Z	8	8	2
$D_{calcd.}$ [g cm^{-3}]	1.552	2.094	1.761
F(000)	2400	1912	710
R(int)	0.0301	0.0439	0.0497
GOF on F^2	1.045	1.032	1.022
R_1[a] [$I > 2\sigma(I)$]	0.0511	0.0518	0.0608
wR_2[b] [$I > 2\sigma(I)$]	0.1365	0.1030	0.1636
Reflections observed/unique	19663/4397	8544/2699	8288/4589
	4	**5**	**6**
Empirical formula	$C_{33}H_{37.5}N_8O_{12.75}Zn_2$	$C_{33}H_{34}N_8O_{13}Zn_2$	$C_{33}H_{37}N_8O_{12}$ Zn_2
Formula weight	880.95	881.42	868.45
Crystal system	monoclinic	triclinic	triclinic
Space group	$P2_1/n$	$P\bar{1}$	$P\bar{1}$
a [Å]	13.4824(7)	10.2489(5)	11.3460(15)
b [Å]	17.0829(6)	10.2912(5)	11.8220(14)
c [Å]	18.1315(6)	17.2945(7)	16.6630(14)
α [°]	90	94.360(4)	107.758(9)
β [°]	110.104(5)	96.728(4)	91.612(9)
γ [°]	90	96.603(4)	112.609(12)
V [Å^3]	3921.6(3)	1792.11(14)	1937.9(4)
Z	4	2	2
$D_{calcd.}$ [g cm^{-3}]	1.492	1.633	1.488
F(000)	1814	904	894
R(int)	0.0721	0.0631	0.0762
GOF on F^2	0.957	0.767	1.004
R_1[a] [$I > 2\sigma(I)$]	0.0508	0.0489	0.0878
wR_2[b] [$I > 2\sigma(I)$]	0.0961	0.0772	0.2167
Reflections observed/unique	16162/7137	11780/6547	13012/6735

[a] $R_1 = \Sigma||F_o| - |F_c||/\Sigma|F_o|$. [b] $wR_2 = |\Sigma w(|F_o|^2 - |F_c|^2)|/\Sigma|w(F_o^2)^2|^{1/2}$.

Crystal Structure Determination: Single crystal XRD data for **1**, **2** and **6** were recorded on an Oxford Diffraction Gemini R Ultra diffractometer with graphite-monochromated Cu-K_α radiation (λ = 1.54184 Å) at 293 K. Single crystal XRD diffraction data for **3**, **4**, and **5** were recorded on an Oxford Diffraction Gemini R Ultra diffractometer with graphite-monochromated Mo-K_α radiation (λ = 0.71073 Å) at 293 K. Absorption corrections were applied with the multiscan technique. All the structures were solved by direct methods with SHELXS-97, and refined by full-matrix least-squares techniques with the SHELXL-97 program.[13] Non-hydrogen atoms of the complexes were refined with anisotropic temperature parameters. The hydrogen atoms attached to carbons were generated geometrically, and refined with a riding model with d(C–H) = 0.93 Å, U_{iso} = 1.2U_{eq}(C) for aromatic H atoms and d(C–H) = 0.97 Å, U_{iso} = 1.5U_{eq}(C) for methylene H atoms. Some water H atoms and hydroxy H atoms were located in the difference Fourier maps and refined as riding atoms with d(O–H) = 0.85–0.89 Å and U_{iso} = 1.5Ueq(O). However, some water H atoms in compounds **4**, **5**, and **6** were not included in the models.

Detailed crystallographic data and structure refinement parameters for these compounds are summarized in Table 1. Selected bond lengths and angles, and hydrogen bond details for the compounds are listed in Tables S1a–S6 (see Supporting Information).

CCDC-784145 (for **1**), -784146 (for **2**), -784147 (for **3**), -784148 (for **4**), -784149 (for **5**), -784150 (for **6**) contain the supplementary crystallographic data for this paper. These data can be obtained free of charge from the Cambridge Crystallographic Data Centre via www.ccdc.cam.ac.uk/data_request/cif.

Supporting Information (see also the footnote on the first page of this article): Selected bond lengths and angles, hydrogen bonds, 2D hydrogen-bond layer in compound **1**, 3D supramolecular network of compound **5**, TGA curves, XRD of compounds **1**–**6**.

Acknowledgments

We thank the Program for Changjiang Scholars and Innovative Research Teams in Chinese Universities, the National Natural Science Foundation of China (grant numbers 21071028, 21001023), the Science Foundation of Jilin Province (grant numbers 20090137, 20100109), the Fundamental Research Funds for the Central Universities, the Specialized Research Fund for the Doctoral Program of Higher Education, the China Postdoctoral Science Foundation (grant numbers 20080431050 and 200801352), and the Training Fund of NENU's Scientific Innovation Project and the Analysis and Testing Foundation of Northeast Normal University for support.

---

[1] a) S. Kitagawa, R. Kitaura, S. Noro, *Angew. Chem. Int. Ed.* **2004**, *43*, 2334–2375; b) Y. E. Cheon, M. P. Suh, *Chem. Eur. J.* **2008**, *14*, 3961–3967; c) J. R. Long, O. M. Yaghi, *Chem. Soc. Rev.* **2009**, *38*, 1213–1214; d) S. Noro, S. Kitagawa, T. Akutagawa, T. Nakamura, *Prog. Polym. Sci.* **2009**, *34*, 240–279; e) F. N. Dai, H. Y. He, D. F. Sun, *J. Am. Chem. Soc.* **2008**, *130*, 14064–14065; f) M. Yoshizawa, J. K. Klosterman, M. Fujita, *Angew. Chem. Int. Ed.* **2009**, *48*, 3418–3438; g) G. Férey, *Chem. Soc. Rev.* **2008**, *37*, 191–214; h) M. O'Keeffe, M. A. Peskov, S. J. Ramsden, O. M. Yaghi, *Acc. Chem. Res.* **2008**, *41*, 1782–1789; i) L. J. Murray, M. Dincă, J. R. Long, *Chem. Soc. Rev.* **2009**, *38*, 1294–1314; j) W. Ki, J. Li, *J. Am. Chem. Soc.* **2008**, *130*, 8114–8115.

[2] a) N. W. Ockwig, O. Delgado-Friedrichs, M. O'Keeffe, O. M. Yaghi, *Acc. Chem. Res.* **2005**, *38*, 176–182; b) S. R. Batten, R. Robson, *Angew. Chem. Int. Ed.* **1998**, *37*, 1460–1494; c) A. J. Blake, N. R. Champness, P. Hubberstey, W.-S. Li, M. A. Withersby, M. Schröder, *Coord. Chem. Rev.* **1999**, *183*, 117–138; d) S. L. James, *Chem. Soc. Rev.* **2003**, *32*, 276–288; e) P. J. Hagrman, D. Hagrman, J. Zubieta, *Angew. Chem. Int. Ed.* **1999**, *38*, 2638–2684; f) O. R. Evans, W. Lin, *Acc. Chem. Res.* **2002**, *35*, 511–522.

[3] a) T. L. Hennigar, D. C. MacQuarrie, P. Losier, R. D. Rogers, M. J. Zaworotko, *Angew. Chem. Int. Ed. Engl.* **1997**, *36*, 972–973; b) X. Meng, Y. Song, H. Hou, H. Han, B. Xiao, Y. Fan, Y. Zhu, *Inorg. Chem.* **2004**, *43*, 3528–3536; c) R. Robson, B. F. Abrahams, S. R. Batten, R. W. Gable, B. F. Hoskins, J. Liu, in: *Supramolecular Architecture*, ACS Publications, Washington, DC, **1992**.

[4] a) S. A. Barnett, N. R. Champness, *Coord. Chem. Rev.* **2003**, *246*, 145–168; b) B. Rather, M. J. Zaworotko, *Chem. Commun.* **2003**, 830–831; c) X.-L. Wang, C. Qin, E.-B. Wang, L. Xu, *Cryst. Growth Des.* **2006**, *6*, 2061–2065.

[5] a) D. Venkataraman, S. Lee, J. S. Moore, P. Zhang, K. A. Hirsch, G. B. Gardner, A. C. Covey, C. L. Prentice, *Chem. Mater.* **1996**, *8*, 2030–2040; b) H. W. Roesky, M. Andruh, *Coord. Chem. Rev.* **2003**, *236*, 91–119; c) M. J. Zaworotko, *Chem. Commun.* **2000**, 1–9.

[6] a) J. Fan, C. Slebodnick, R. Angel, B. E. Hanson, *Inorg. Chem.* **2005**, *44*, 552–558; b) L. Carlucci, G. Ciani, D. M. Proserpio, *Chem. Commun.* **2004**, 380–381; c) J. Fan, G. T. Yee, G. Wang, B. E. Hanson, *Inorg. Chem.* **2006**, *45*, 599–608.

[7] a) H.-Y. Bai, J.-F. Ma, J. Yang, Y.-Y. Liu, H. Wu, J. C. Ma, *Cryst. Growth Des.* **2010**, *10*, 995–1016; b) H.-Y. Bai, J.-F. Ma, J. Yang, L.-P. Zhang, J.-C. Ma, Y.-Y. Liu, *Cryst. Growth Des.* **2010**, *10*, 1946–1959.

[8] a) J. Fan, C. Slebodnick, D. Troya, R. Angel, B. E. Hanson, *Inorg. Chem.* **2005**, *44*, 2719–2727; b) Z.-E. Lin, W. Fan, F. Gao, N. Chino, T. Yokoi, T. Okubo, *Cryst. Growth Des.* **2006**, *6*, 2435–2437; c) J. Li, L. Li, J. Liang, P. Chen, J. Yu, Y. Xu, R. Xu, *Cryst. Growth Des.* **2008**, *8*, 2318–2323; d) L. Chen, X. Bu, *Chem. Mater.* **2006**, *18*, 1857–1960; e) W. T. A. Harrison, R. M. Yeates, M. L. F. Phillips, T. M. Nenoff, *Inorg. Chem.* **2003**, *42*, 1493–1498; f) J. A. Johnstone, W. T. A. Harrison, *Inorg. Chem.* **2004**, *43*, 4567–4569; g) S. Mandal, S. Natarajan, *Inorg. Chem.* **2008**, *47*, 5304–5313; h) Z. Lin, H. P. Nayek, S. Dehnen, *Inorg. Chem.* **2009**, *48*, 3517–3519; i) L. Chen, X. Bu, *Inorg. Chem.* **2006**, *45*, 4654–4660.

[9] a) Q. Wu, M. Esteghamatian, N.-X. Hu, Z. Popovic, G. Enright, Y. Tao, M. D'Iorio, S. Wang, *Chem. Mater.* **2000**, *12*, 79–83; b) J. E. McGarrah, Y.-J. Kim, M. Hissler, R. Eisenberg, *Inorg. Chem.* **2001**, *40*, 4510–4511; c) G. D. Santis, L. Fabbrizzi, M. Licchelli, A. Poggi, A. Taglietti, *Angew. Chem. Int. Ed. Engl.* **1996**, *35*, 202–204.

[10] a) X. Shi, G. Zhu, Q. Fang, G. Wu, G. Tian, R. Wang, D. Zhang, M. Xue, S. Qiu, *Eur. J. Inorg. Chem.* **2004**, 185–191; b) X.-M. Zhang, M.-L. Tong, M.-L. Gong, X.-M. Chen, *Eur. J. Inorg. Chem.* **2003**, 138–142; c) G. Tian, G. Zhu, Q. Fang, X. Guo, M. Xue, J. Sun, S. Qiu, *J. Mol. Struct.* **2006**, *787*, 45–49.

[11] a) W. Chen, J.-Y. Wang, C. Chen, Q. Yue, H.-M. Yuan, J.-S. Chen, S.-N. Wang, *Inorg. Chem.* **2003**, *42*, 944–946; b) J. Yang, Q. Yue, G.-D. Li, J.-J. Cao, G.-H. Li, J.-S. Chen, *Inorg. Chem.* **2006**, *45*, 2857–2865; c) A. Thirumurugan, S. Natarajan, *Dalton Trans.* **2004**, 2923–2928; d) X.-J. Zheng, L.-P. Jin, S. Gao, S. Z. Lu, *New J. Chem.* **2005**, *29*, 798–791; e) X.-J. Zheng, L.-P. Jin, S. Gao, *Inorg. Chem.* **2004**, *43*, 1600–1602.

[12] X. Shi, G. Zhu, X. Wang, G. Li, Q. Fang, G. Wu, G. Tian, M. Xue, X. Zhao, R. Wang, S. Qiu, *Cryst. Growth Des.* **2005**, *5*, 207–213.

[13] G. M. Sheldrick, *Acta Crystallogr., Sect. A* **2008**, *64*, 112–122.

Received: July 14, 2010